STROMAL CELL DIVERSITY IN TUMOR MICROENVIRONMENT PROMOTE INVASION OF ORAL SQUAMOUS CELL CARCINOMA

Omneya Mohamed Wahba* *and* Engy Ahmed Youssef Mourad**

ABSTRACT

Background and objectives: Epithelial neoplastic cells only prosper in aberrant microenvironmental conditions. That aberrant environment contains an altered extracellular matrix and multiple stromal cells including, fibroblasts, macrophages, and endothelial cells. In parallel with neoplastic cells, the previous cell types have a pivotal role in tumor pathogenesis and progression. The current study evaluated changes in stromal cells in the tumor microenvironment in patients diagnosed with oral epithelial dysplasia (OED) and oral squamous cell carcinoma (OSCC).

Method: Thirty-six archival OED and 83 archival OSCC cases were included in our research. Immunohistochemistry was performed for α-SMA, CD31, and CD163. Macrophage and Fibroblast counts were performed manually. We also morphologically determined the microvessel density (MVD).

Results: In different types of epithelial dysplasia (mild, moderate, and severe), the number of stromal cells that express α-SMA, CD31, and CD163 increased from mild to severe epithelial dysplasia. As well, in different variants of oral squamous cell carcinoma (well, moderate, and poorly), there was a significant difference in stromal cells that express α-SMA, CD31 and CD163.

Conclusion: These findings reveal that changes in stromal cells beneath oral epithelial dysplasia and in OSCC stroma might play a potential regulatory role in OSCC invasion as well as progression.

KEYWORDS: Stromal Cells, Tumor microenvironment, CD163, Oral squamous cell carcinoma.

* Assistant Professor, Pathologist, Department of Oral Pathology, Faculty of Dental & Oral Medicine, Kafr El-Shiekh University, Kafr El-Shiekh, Egypt.
** Lecturer, Pathologist, Department of Oral Pathology, Faculty of Dental & Oral Medicine, Kafr El-Shiekh University, Kafr El-Shiekh, Egypt.

INTRODUCTION

The tumor microenvironment consists of both cells and the extracellular matrix (ECM) that surround tumor cells [1]. Not only do neoplasms affect the surrounding microenvironment via the release of extracellular signals that induce angiogenesis and immune system tolerance, but the immune cells in that environment could also greatly affect the growth and progression of these neoplasms. So, the stroma of neoplastic tissues has a crucial role in tumor progression [2].

Oral squamous cell carcinoma (OSCC) accounts for 90% of the malignant neoplasms affecting the oral cavity, making it the most common malignant oral neoplasm [3]. That neoplasm has a bad prognosis, as its survival rate does not exceed 50%, despite the great advances in the diagnosis and therapeutics achieved in the oncology field. Therefore, it is crucial for physicians to early detect and diagnose precancerous lesions that predispose to OSCC in order to prevent its progression into cancer and enhance patients' outcomes [4,5].

Cancer development is associated with particular changes that occur in the epithelium and its underlying stroma. In the cancer environment, the underlying stroma becomes reactive, leading to the secretion of several cytokines, such as transforming growth factor beta-1, from the neoplastic cells. These cytokines mediate the differentiation of normal fibroblasts in the stroma into cancer-associated fibroblasts (CAF). In addition, the number of blood cells and inflammatory cells increases. Moreover, the expression of epithelial markers like cadherins decreases, whereas that of mesenchymal markers like vimentin increases. Matrix metalloproteases are also secreted. The previous changes lead to remodeling of the extracellular matrix and subsequent tumor growth[6].

Tumor-associated macrophages (TAMs) represent a major inflammatory component in the neoplastic tissue, as they occupy a significant portion of the surrounding stroma and are mainly present just near the neoplastic cells. These cells are polarized to the M2 phenotype, and they enhance neoplastic cell proliferation by evading the immune system [7]. Additionally, there is a misbalance in the angiogenesis process in malignant neoplasms, as there is a significant rise in pro-angiogenic factors while inhibitory factors decrease. That imbalance is in favor of tumor vascularization and growth [8].

Although there is evidence that the stroma in the neoplastic microenvironment can influence the progression of multiple types of cancer, similar data on OSCC is still limited. Therefore, our study was conducted to reveal the changes in stromal cells in the OSCC stroma as well as beneath oral epithelial dysplasia (OED).

Methodology

Selection of cases

Our research was conducted in the Oral Pathology departments of both Tanta and Alexandria Universities over a five-year duration, from January 2018 to December 2022. Eighty- three archival OSCC cases and 36 OED cases were collected. Two expert pathologists blindly confirmed the diagnosis. We included OSCC patients, whatever the degree of differentiation (well-differentiated 38 cases, moderately-differentiated 26 cases, and poorly-differentiated 19 cases). OED cases were included, whatever the degree of dysplasia (mild 10 cases, moderate 12 cases, and severe 14 cases). Normal oral epithelium was collected from 20 gingivectomy cases as a control group. Our research was approved by the local ethical scientific committee of the Faculty of Dentistry, Kafr El-shiekh University (KD /24/21).

All patients diagnosed with primary OSCC were included, while patients with nodal or distant metastases were excluded. We intended to include pathological sections with sufficient tissue and

proper fixation technique, while sections with insufficient tissue, hemorrhage, inflammation, and incisional biopsies were excluded.

Conventional staining with hematoxylin and eosin

Fixation of the selected samples was done via formalin (10%), followed by its processing in paraffin. Serial 5-μm sections were obtained from the paraffin blocks for hematoxylin, eosin.

Immunohistochemistry

In our study, we used three types of mouse monoclonal antibodies that were designed against human CD31 (JC70A, IgG1), alpha smooth muscle actin (1A4, IgG2a), and human CD163 (10D6, IgG1). The first two antibodies were purchased from Dako (Glostrup, Denmark), whereas the latter was purchased from Novocastra (New Castle, UK). The ChemMate EnvisionTM system (Dako) was used for IHC. Thick sections (4 μm) were prepared for IHC staining. The gathered sections were autoclaved in a citrate buffer (pH 6) at 121 C for ten minutes to prepare them for CD163 and CD31, while α SMA sections were also autoclaved at the same temperature and for the same duration, but a Tris-EDTA buffer was used (pH 9.0). For blocking the activity of endogenous peroxidase, we treated the collected sections with $H2O2$ (0.3%) in methanol for half an hour at room temperature. For blocking non-specific protein binding sites, we incubated the sections for one hour at room temperature in 5% milk protein in 0.01 M phosphate-buffered saline (PBS, pH 7.4) containing Triton X-100 0.05% (T-PBS). After that, the sections were incubated at 4 °C over night with the primary antibodies diluted at 1:100 (CD163, CD31, and α-SMA) in PBS. When the overnight incubation ended, the Envision reagents were used to incubate the sections for one hour at room temperature. Reaction products were visualized with 0.02% 3, 30-diaminobenzidine in a 0.05 M Tris-HCl buffer (pH 7.6) containing $H2O2$ (0.005%). Finally, counterstaining of the sections

was done via hematoxylin. For the control group, we used preimmune IgGs rather than the primary antibodies.

Assessment of immunohistochemical staining

The presence of membranous, cytoplasmic, or nuclear brown-colored reaction was considered a positive reaction. The intensity of the immunostaining was classified as negative, weak, moderate or strong from three fields in blinded analysis performed by two experienced research associates using a conventional light microscope followed by image analysis using the Image J software (version 4.10.03, Nikon, Tokyo, Japan).

Cell counting for CD163+ macrophages and α-SMA+ fibroblasts

Using a 40x objective lens, three separate OSCC and OED stromal fields were randomly chosen at higher magnification after tissue sections were examined at lower magnification. A Nikon Eclipse microscope equipped with a Nikon DXM1200C digital camera (Nikon, Japan) was used to obtain photographs for the representative regions for each category. Mononucleated macrophages positive for CD163 and for α-SMA+ fibroblasts were manually counted in the same unit field of the stromal space (0.25 × 0.25 mm) on serial sections. We excluded small positive-stained cells (relative to the circulating monocytes) from counting [9].

Counting of Microvessel density (MVD)

Three hotspot sites were photographed at high magnification using a 20x objective lens after the entire section was low-magnified scanned to find the areas that were highly vascularized (hot spots). We manually counted blood vessels positive for CD31 in a unit field of 0.54 mm^2 and considered them as MVDs. After that, the average was calculated, and the Anova was used to reveal any significant statistical difference [9].

Statistical analysis

Using SPSS version 20, the data obtained for the current study were gathered, tabulated, and statistically evaluated. The Chi-square test was employed to compare qualitative data. Using mean, standard deviation, and confidence intervals, quantitative data were summarized and compared using Student's test or one-way analysis of variance test. The tests of the statistical analyses were considered significant if the p-value was less than 0.05.

RESULTS

Normal Epithelia

In normal epithelia obtained from gingivectomy cases, stromal cells (fibroblasts, α-SMA+; Mean ± SD = 30.00 ± 7.48), (endothelial cells, CD31+; Mean ± SD = 5.50 ± 1.62) and (Macrophages, CD163+; Mean ± SD = 3.00 ± 1.35) were very few in number beneath the surface epithelium (data not shown).

Mild epithelial dysplasia

In mild epithelial dysplasia, there were the changes in the lower third of the epithelium including cytological atypia and hyperchromatism (Fig. 1A). Immunostaining of α-SMA showed weak brown staining only in blood vessel walls, less immunostaining was observed in stromal cells (Mean ± SD = 37.30 ± 8.45) (Fig. 1D). Very few numbers of CD31+ blood vessels were seen beneath the dysplastic epithelium (Mean ± SD = 5.70 ± 1.25) (Fig. 1G). Macrophages that were CD163+ were not observed beneath dysplastic epithelium (Mean ± SD = 5.10 ± 2.23) (Fig. 1J).

Moderate epithelial dysplasia

In moderate epithelial dysplasia where there were dysplastic changes extending into the middle third of the epithelium (Fig. 1B). Immunostaining of α-SMA showed weak brown staining only in blood vessel walls, less immunostaining was observed in

stromal cells (Mean ± SD = 44.75 ± 12.49) (Fig. 1E). Very few numbers of CD31+ blood vessels were seen beneath dysplastic epithelium (Mean ± SD = 7.83 ± 2.79) (Fig. 1H). Few macrophages that were CD163+ were observed beneath dysplastic epithelium (Mean ± SD = 10.17 ± 3.61) (Fig. 1K).

Severe epithelium dysplasia

In severe epithelial dysplasia where there were architectural changes that exceeded two thirds of the epithelium that is associated with cytological atypia (Fig. 1C). Stromal expression of α-SMA in stromal cells was observed as well as in blood vessel walls (Mean ± SD = 56.07 ± 11.03) (Fig. 1F). In addition, there was an increase in the number of CD31+ blood vessels in the stroma more than was observed in mild and moderate epithelial dysplasia (Mean ± SD = 13.57 ± 4.55) (Fig. 1I). There were increased number of macrophages that were CD163+ were observed beneath dysplastic epithelium (Mean ± SD = 21.93 ± 5.88) (Fig. 1L).

Well Differentiated Squamous Cell Carcinoma

In well-differentiated OSCC, where there were invading nests of malignant epithelial cells with abundant eosinophilic cytoplasm and marked extents of cell keratinization (keratin pearls) (Fig. 2A). Increased expression of α-SMA in blood vessel walls and number of stromal fibroblasts (Mean ± SD = 92.65 ± 22.81) (Fig. 2D). There was a significant increase in CD31+ blood vessels (Mean ± SD = 23.24 ± 4.65) (Fig 2G) as well as increased number of macrophages that were CD163+ (Mean ± SD = 47.11 ± 10.53) (Fig. 2J)

Moderate Differentiated Squamous Cell Carcinoma

In moderate differentiated OSCC, where there were islands of malignant epithelial cells that infiltrated the OSCC stroma with various nuclear shapes and sizes, a less extent of cell keratinization, and multiple atypical mitoses (Fig. 2B). Enriched

number of α-SMA+ fibroblasts was noted (Mean ± SD = 110.31 ± 28.42) (Fig. 2E). There was increased in the expression of CD31+ endothelial cells in peri-tumoral and intra-tumoral stroma (Mean ± SD = 22.04 ± 3.10) (Fig. 2H) as well as increased number of macrophages that were CD163+ (Mean ± SD = 48.04 ± 8.51) (Fig. 2K)

Poorly Differentiated Squamous Cell Carcinoma

In poorly differentiated OSCC, where there were streaming malignant epithelial cells of various shapes and sizes associated with atypical mitotic figures, and no cell keratinization was observed.

(Fig. 2C). Increased numbers of α-SMA+ fibroblasts were noted (Mean ± SD = 108.79 ± 28.68) (Fig. 2F). There was an increase in the expression of CD31+ endothelial cells in peri-tumoral and intra-tumoral stroma (Mean ± SD = 23.58 ± 3.31) (Fig. 2I) as well as an increased number of macrophages that were CD163+ (Mean ± SD = 56.63 ± 10.39) (Fig. 2L).

In different grades of epithelial dysplasia as well as in different variants of oral squamous cell carcinoma, there was a significant difference in the expression of α-SMA, CD31, and CD163 (p value < 0.001) (Fig. 3).
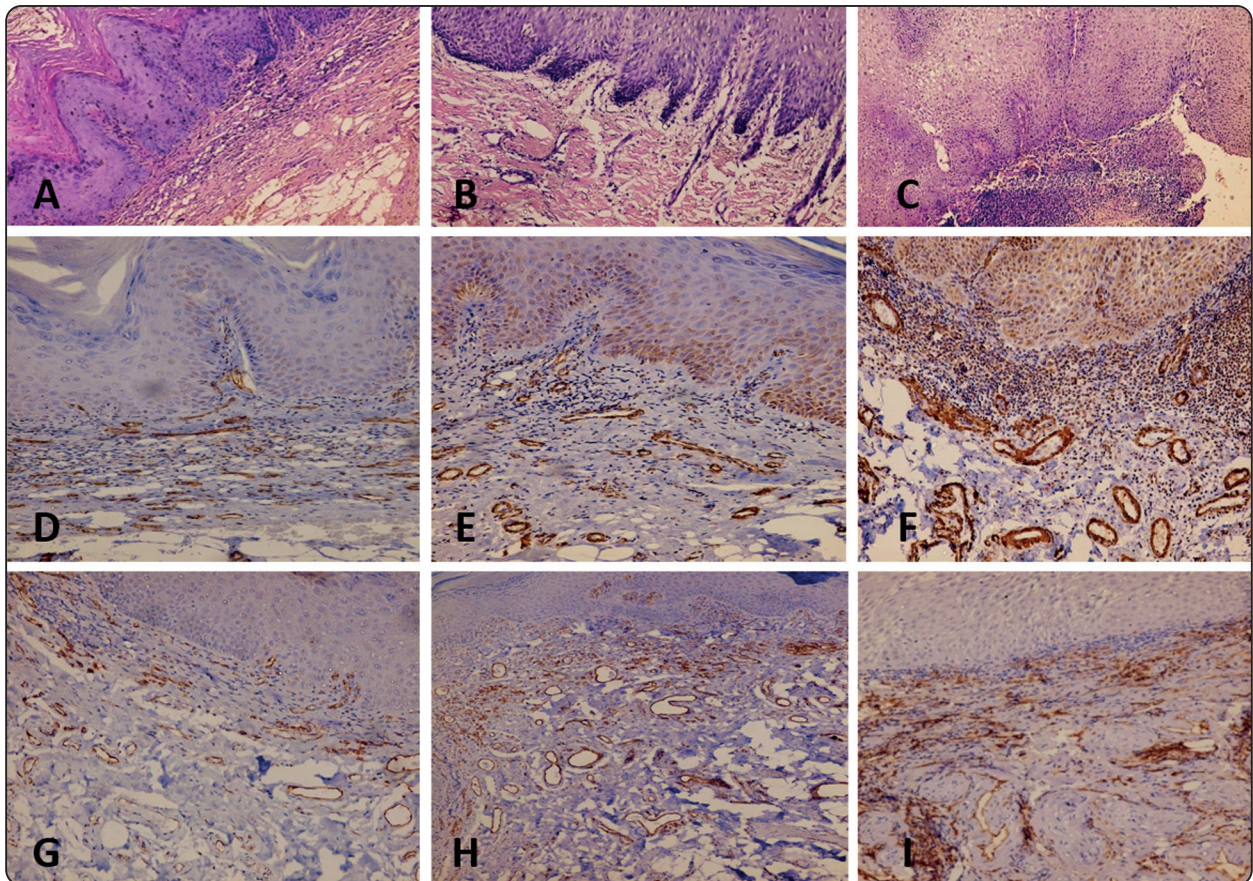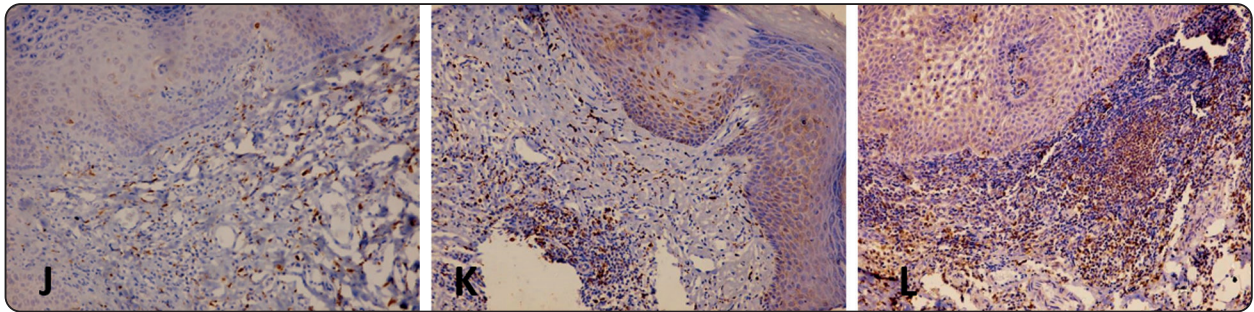
Fig. (1) Stromal cell beneath epithelial dysplasia. In mild epithelial dysplasia; where there were architectural changes in the lower third of the epithelium including cytological atypia and hyperchromatism (Fig. 1A). Immunostaining of α-SMA showed weak brown staining only in blood vessel walls (Fig. 1D). Very few numbers of CD31+ blood vessels were seen beneath dysplastic epithelium (Fig. 1G). Very few macrophages that were CD163+ were observed beneath dysplastic epithelium (Fig. 1J). In moderate epithelial dysplasia where there were architectural changes extending into the middle third of the epithelium (Fig. 1B). Immunostaining of α-SMA showed weak brown staining only in blood vessel walls, no immunostaining was observed in stromal cells (Fig. 1E). Very few numbers of CD31+ blood vessels were seen beneath dysplastic epithelium (Fig. 1H). Few macrophages that were CD163+ were observed beneath dysplastic epithelium (Fig. 1K). In severe epithelial dysplasia where there were architectural disturbances in greater than two thirds of the epithelium with cytological atypia (Fig. 1C). Emergence of α-SMA+ stromal cells was observed in the well as in blood vessels walls (Fig. 1F). In addition, there were an increase in the number of CD31+ blood vessels in the stroma more than observed in mild and moderate epithelial dysplasia (Fig. 1I). There were increased number of macrophages that were CD163+ were observed beneath dysplastic epithelium (Fig. 1L). Hematoxylin and eosin (HE) (A-C) and immunoperoxidase stains for α-SMA (D-F)); CD31 (G-I); CD163 (J-L) × 200.
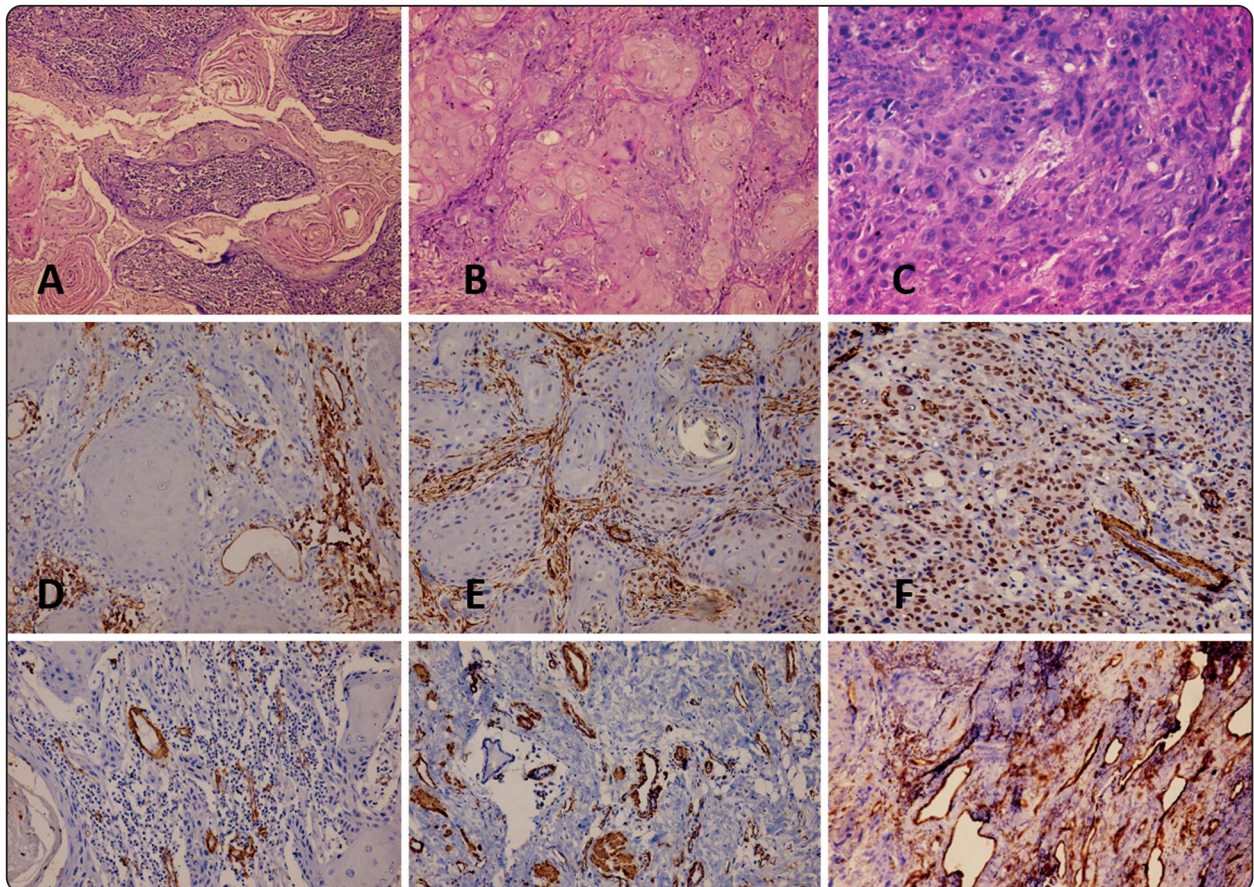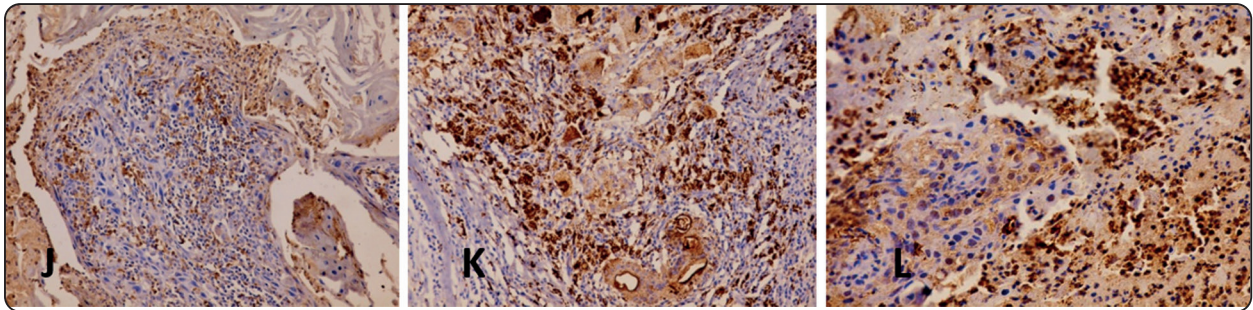
Fig. (2) Stromal cell in OSCC. In well differentiated OSCC where there were invading nests of malignant squamous epithelial cells, these malignant cells are often large with abundant eosinophilic cytoplasm and a large vesicular nucleus also variable keratinization (keratin pearls) were noted (Fig. 2A). Immunostaining of α-SMA, the expression of α-SMA in blood vessel walls and stromal myofibroblasts in well differentiated squamous cell carcinoma was nearly similar to its expression in severe epithelial dysplasia, the pattern that was seen in moderate type was network or spindle pattern (Fig. 2D). Immunostaining of CD31, there was a significant increase between CD31 expression in well differentiated squamous cell carcinoma and all types of the epithelial dysplasia (Fig 2G). Immunostaining of CD163, intensity of stromal macrophages were more than its intensity in epithelial dysplasia (Fig. 2J) In moderate differentiated OSCC where there were organized islands of neoplastic atypical epithelial cells which infiltrated the tumoral stroma. The nuclei of the neoplastic cells had different shapes and sizes (cellular and nuclear pleomorphism), also the cells showed rare intercellular bridges, hyperchromatic nuclei, few individual cell keratinization and multiple atypical mitosis. The stroma was rich in inflammatory cells and angiogenic vessels (Fig. 2B). Immunostaining of α-SMA, positive staining of stromal myofibroblasts to α-SMA showed spindle and network pattern and was significantly higher than well differentiated type (Fig. 2E). Immunostaining of CD31, increase in the expression of CD31 by the endothelial cells in peri-tumoral and intra-tumoral stroma (Fig. 2H). Immunostaining of CD163, staining of stromal macrophages was significantly higher than that in well differentiated squamous cell carcinoma (Fig. 2K) In poorly differentiated OSCC where there were cellular cords, islands or epithelioid like cells of various shapes and sizes with a different design from the normal epithelium. Increase in the atypical mitotic figures of the malignant cells which are highly hyperchromatic and no keratin was observed. The stroma was heavily infiltrated by chronic inflammatory cells (Fig. 2C). Immunostaining of α-SMA, stromal myofibroblasts showed focal pattern staining of α-SMA and also showed the highest expression among all types of oral squamous cell carcinoma and oral dysplasia (Fig. 2F). Immunostaining of CD31, staining of blood vessels in tumoral stroma was higher than its expression in well and moderate differentiated squamous cell carcinoma (Fig. 2I). Immunostaining of CD163, tumor associated macrophages showed the highest staining (Fig. 2L). Hematoxylin and eosin (HE) (A-C) and immunoperoxidase stains for α-SMA (D-F)); CD31 (G-I); CD163 (J-L) × 200.
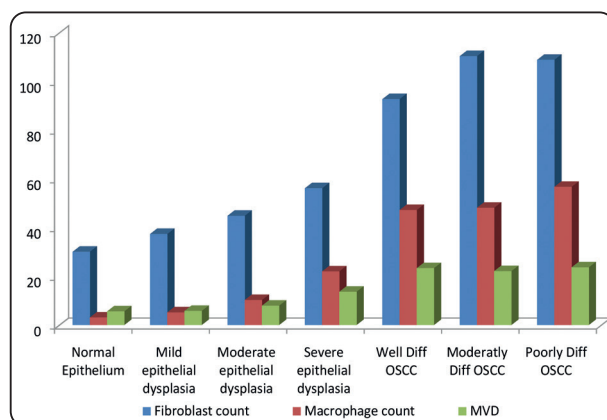

Fig. (3) In different grades of epithelial dysplasia as well as in different variants of oral squamous cell carcinoma, there was significant difference in the expression of α-SMA, CD31 and CD163 (p value < 0.001).

DISCUSSION

Epithelial neoplastic cells only prosper in aberrant microenvironmental conditions. That aberrant environment contains an altered extracellular matrix and multiple stromal cells including, fibroblasts, macrophages, and endothelial cells [1]. The stroma itself may form a variable portion of the tumor, reaching up to 90%. Previous data suggest that stroma reacts to neoplastic cells similarly to how it might respond to a wound[10]. In addition, reciprocal interactions between stromal cells and cancer cells result in subsequent cancer initiation, progression, and metastasis [8]

Due to their capacity to alter the extracellular matrix, CAFs play a significant role in tumor invasion, development, and metastasis [11]. Considering the results obtained in this study, the number of α-SMA+ fibroblasts in the OSCC stroma was greater than seen in epithelial dysplasia, which was in accordance with the role of CAFs in the invasive behavior of OSCC. Significant differences in the expression of α-SMA from OED to OSCC (p < 0.001) were noted. Several previous studies observed a significantly increased number of CAFS in moderately differentiated and poorly differentiated OSCC as compared to well-differentiated OSCC and different grades of OED. These results might highlight a point in the invasive stage of OSCC where the conversion of fibroblasts to CAFs is initiated [12-15].

Angiogenesis or neovascularization is essential for the development and progression of malignant tumors [16]. Actually, no solid tumor can expand beyond 2-3 mm in diameter without developing a self-sufficient blood supply. In this study, there was a significant difference when comparing MVD between different types of OED and different grades of OSCC (p < 0.001), which supports Folkman's concept that stated that tumor growth and progression is dependent on the angiogenesis process. In addition, as the abnormal tissue transforms from dysplasia into carcinoma, its metabolic needs increase. These metabolic demands are met by the increased proangiogenic factors secreted from the tumor cells with the aid of the surrounding stroma [17].

Other clarifications to the enhanced CD31 expression had been attributed to the ability of the CD31 to alter the cytoskeleton of the endothelial cells, leading to their proliferation, migration, and adhesion and in turn, activation of tumor-induced angiogenesis[18]. Studies on CD31 expression revealed no significant difference in the expression of CD31 between fibromas, OEDs, and OSCCs, as well as in normal mucosa, adenoma and adenocarcinoma of colon. It had been proposed that these conflicting results could be attributed to the use of different markers and methods in the micro vessel counting, antigenic retrieval, and inter-observer variations; that all of these factors affect the assessment of MVD [19]. Moreover, the inability of CD31 to distinguish newly formed tumoral blood vessels from normal pre-existing ones in both neoplastic and non-neoplastic tissues [20].

In this study, we selected CD163 expression for M2 polarized macrophages (both CD68+ and CD163+) and we found that CD163+ expressions in the various OSCC and OED groups are highly significant (p < 0.001). These findings indicate that the recruitment of TAMs and their polarization from M1 (CD68+/CD163-) to M2 (CD68+/CD163+) macrophages has a potential role in tumor behavior. Studies that support our results stated that the expression of CD163 is concomitant with TAMs and is higher in OSCC than that in OED, and the higher the grade of dysplasia and malignancy, the higher the expression of CD163+ macrophages. This finding indicates that TAMs play an important role in providing suitable conditions for the progression of tumors and cancer and are associated with poor prognosis [21,22]. In contrast to our findings, other studies revealed that there is no significant difference among the three groups of OSCC and OED in terms of CD68 staining. These opposite results might be explained because they restricted the use of CD68 as a pan-macrophage marker but not CD163 [23,24].

In conclusion, most cancer studies have focused on finding new diagnostic and prognostic indicators for early tumor detection, progression, and metastasis. Such markers might be used as targets for anti-cancer treatments, which would eventually lower the morbidity and mortality rates related to cancer. Further detailed investigations should be performed to elucidate the exact mechanism by which stromal cells are involved in the process of OSCC progression.

REFERENCES

1. Bissell MJ, Radisky D. Putting tumors in context. Nat Rev Cancer. 2001; 1:46–54.

2. Korneev KV, Atretkhany KN, Drutskaya MS, Grivennikov SI, Kuprash DV, Nedospasov SA. "TLR-signaling and proinflammatory cytokines as drivers of tumorigenesis". Cytokine. 2017; 89: 127–35.

3. A Smitha, Kavita Rao, H S Umadevi, T Smitha, H S Sheethal, M A Vidya. Immunohistochemical study of α-smooth muscle actin expression in oral leukoplakia and oral squamous cell carcinoma. J Oral Maxillofac Pathol. 2019; 23(1): 59–64.

4. Gillenwater A, Papadimitrakopoulou V, Kortum RR. Oral premalignancy: new methods of detection and treatment. Curr Oncol Rep. 2006; 8:146–54.

5. Lamouille S, Xu J, Derynck R. Molecular mechanisms of epithelial-mesenchymal transition. Nat Rev Mol Cell Biol. 2014; 15(3):178–96.

6. Kanupriya Gupta, Rashmi Merged, Jatin Gupta. Evaluation of stromal myofibroblasts in oral leukoplakia, oral submucous fibrosis, and oral squamous cell carcinoma - an immunohistochemical study. Journal of Cancer Research and Therapeutics.2015; 11(4): 893-8.

7. Zhang W, Wang L, Zhou D, Cui Q, Zhao D, Wu Y. "Expression of tumor-associated macrophages and vascular endothelial growth factor correlates with poor prognosis of peripheral T-cell lymphoma, not otherwise specified". Leukemia & Lymphoma. 2011; 52 (1): 46–52.

8. Pujari R, Vanaki S, Puranik R, et al. Histomorphometric analysis of vascularity in normal buccal mucosa, leukoplakia, and squamous cell carcinoma of buccal mucosa. J Oral Maxillofac Pathol. 2013; 17(3):334–9.

9. Essa, A. A., Yamazaki, M. & Maruyama, S. Tumour-associated macrophages are recruited and differentiated in the neoplastic stroma of oral squamous cell carcinoma. Pathology48, 219–227 (2016).

10. Neeta Bagul, Souparna Roy, Anjali Ganjre, Rahul Kathariya, Aishwarya Meher, Pratibha Singh. Quantitative Assessment of Tumor Associated Macrophages in Head and Neck Squamous Cell Carcinoma Using CD68 Marker: An Immunohistochemical Study. Journal of Clinical and Diagnostic Research. 2016;10(4): ZC81 – ZC 84.

11. Mrinal V. Shete, Revati S. Deshmukh, Tejas Kulkarni, Anagha V. Shete, Prasad Karande,, Pratik Hande. Myofi-broblasts as important diagnostic and prognostic indicators of oral squamous cell carcinoma: An immunohistochemical study in normal oral mucosa, epithelial dysplasia, and oral squamous cell carcinoma. J Carcinog. 2020; 19: 1.

12. Khalid A, Siddiqui S, Faizi N, Hassan J, Nehal N, Siddiqui A. Role of stromal myofibroblasts in the progression of oral lesions from dysplasia to invasive carcinoma. Indian J Med Paediatr Oncol. 2019; 40:536–41.

13. Smitha A, Rao K, Umadevi HS, Smitha T, Sheethal HS, Vidya MA. Immunohistochemical study of α-smooth muscle actin expression in oral leukoplakia and oral squamous cell carcinoma. J Oral Maxillofac Pathol. 2019; 23:59–64.

14. Rodrigues PC, Miguel MCD, Aquino SND, Fonseca FP, Silva ARS, Leme AFP, et al. Stromal myofibroblasts in potentially malignant and malignant lesions of the oral cavity. Oncol Lett. 2015; 9:667–70.

15. Kapse SC, Rathod N, Baad R, Mandlik J, Sharma AS, Bommanavar S. Quantitative assessment of myofibroblast in severe dysplasia, microinvasion and oral squamous cell carcinoma: An immunohistochemical study. J Contemp Dent Pract. 2013; 14:34–8.

16. Amina Fouad Farag, Rehab Fawzi Kasem, Nahed Emad El-Din Abo-Azma, Mohsen Kazem Abd El-Latif. Evaluation of Angiogenesis in Oral Epithelial Dysplasia and Oral Squamous Cell Carcinmoa: An Immunohistochemical Comparison between Anti-CD105 and Anti-CD31 Antibodies. Int. J. Adv. Res.2018; 6(1):338-347.

17. Lertkiatmongkol P., Liaoa D., Meib H., Hub Y., Newmana P. Endothelial functions of platelet/endothelial cell adhesion molecule-1 (CD31). Curr. Opin. Hematol. 2016; 23(3):253-9.

18. De Oliveira M., Pereira Gomes E., Pereira C., de Souza L., Barros L., Mendes D., et al. Prognostic value of micro vessel density and p53 expression on the locoregional metastasis and survival of the patients with head and neck squamous cell carcinoma. Appl. Immunohistochem. Mol. Morphol.2013; 21(5):444-51.

19. Fernández A., Fernández J., Marshall M., Martínez R., Niklander S., Haidar Z. Difference in EGFR expression and mean vascular density in normal oral mucosa, oral epithelial dysplasia and oral squamous cell carcinoma. J. Oral Res. 2017;6(2):39-45.

20. Basilio de Oliveira R. and Pannain V. Prognostic angiogenic markers (Endoglin, VEGF, CD31) and tumor

cell proliferation (Ki67) for gastrointestinal stromal tumors. World J. Gastroenterol.2015 ;21(22):6924-30.

21. He KF, Zhang L, Huang CF, Ma SR, Wang YF, Wang WM, et al. CD163+ tumor-associated macrophages correlated with poor prognosis and cancer stem cells in oral squamous cell carcinoma. Biomed Res Int. 2014; 838632.

22. Chawla H, Urs AB, Augustine J. Association of macrophages with angiogenesis in oral epithelial dysplasia, oral verrucous carcinoma, and oral squamous cell carcinoma: an immunohistochemical study. Appl Immunohistochem Mol Morphol. 2017; 25(3):203- 8.

23. Shadi Saghafi, Reza Zare Mahmoud Abadi, Samira Basir Shabestari, Shaygan Fazel, Iman Shirinbak. Angiogenesis and Tumor-Associated Macrophages in Different Grades of Oral Squamous Cell Carcinoma, Verrucous Carcinoma and Epithelial Dysplasia via Immunohistochemical Assessment of Expression of CD34 and CD68 Markers. Journal of Kerman University of Medical Sciences. 2019; 26 (2): 110-9.

24. El-Rouby DH. Association of macrophages with angiogenesis in oral verrucous and squamous cell carcinomas. J Oral Pathol Med. 2010; 39(7):559-64.